

In Situ Spectroscopic, Electrochemical, and Theoretical Studies of the Photoinduced Host–Guest Electron Transfer that Precedes Unusual Host-Mediated Alkane Photooxidation

Yuji Furutani,[†] Hideki Kandori,^{*,†} Masaki Kawano,^{*,‡} Koji Nakabayashi,[‡]
Michito Yoshizawa,^{‡,§} and Makoto Fujita^{*,‡}

Department of Frontier Materials, Nagoya Institute of Technology, Showa-ku, Nagoya 466-8555, Japan, Department of Applied Chemistry, School of Engineering, The University of Tokyo, and JST, CREST, 7-3-1 Hongo, Bunkyo-ku, Tokyo 113-8656, Japan

Received November 13, 2008; E-mail: mfujita@appchem.t.u-tokyo.ac.jp

Abstract: In the unusual photooxidation of alkanes within the cavity of a self-assembled M_6L_4 cage complex (**1**), the proposed reaction mechanism involves the generation of the host anion radical and guest cation radical via guest-to-host photoinduced electron transfer (PET). In the present study, the postulated host anion radical was elucidated by in situ IR spectroscopy. The difference IR spectrum before and after the irradiation of the clathrate complex $1a \supset (2)_4$ (**2** = adamantane) features a dominant negative peak at $\sim 1500\text{ cm}^{-1}$, which is attributed to the decrease in the C=N stretching vibration and thus indicative of the structural change in the triazine core of the cage. Electrochemical measurements and theoretical calculations show the remarkably great electron-accepting ability of the triazine core. These results strongly support the proposal of guest-to-host PET.

Introduction

Photoinduced electron transfer (PET) is an important process in the early stages of photosynthesis that converts solar energy to chemical energy.¹ While there are many reports on PET, reports where PET is followed by chemical transformation are much less common.² Previously, some of us reported the photooxidation of alkanes within the cavity of self-assembled cage **1**.³ The proposed mechanism in this reaction requires PET from the guest to the host (Figure 1). However, no direct evidence for the PET step was available. Here we report that in situ IR spectroscopy coupled with electrochemical measurements and theoretical calculations clearly shows the generation of the host anion radical species resulting from guest-to-host PET. In this process, the extremely electron-deficient triazine panel of the host acts as an electron acceptor. The present results confirm that the cage **1** is not an innocent reaction vessel but provides an electronically altered reaction field that promotes chemical reactions via PET.⁴

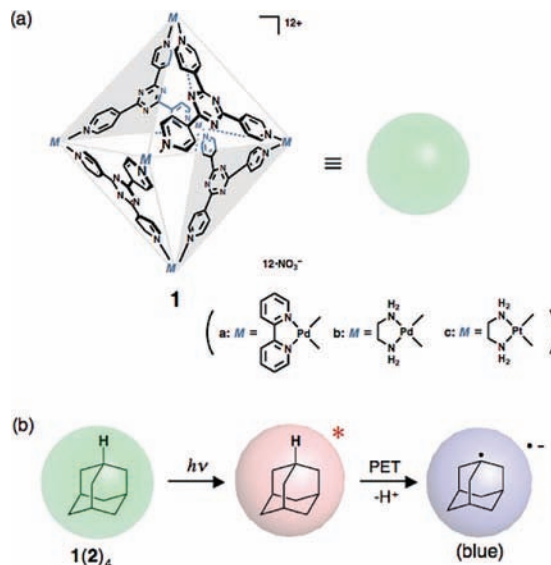


Figure 1. (a) Structure of cage **1**. (b) Proposed PET mechanism for the photooxidation of adamantane (**2**) in the cavity of **1**. Four adamantane molecules are enclathrated, but only one is converted to adamantane radical via PET. The generated radical is trapped by H_2O or O_2 to give oxidized product.

Previous Work. Photolysis of $1 \supset (2)_4$ (**2** = adamantane) by a high-pressure mercury lamp in a Pyrex tube produced two

[†] Nagoya Institute of Technology.

[‡] The University of Tokyo and JST.

[§] Present address: Tokyo Institute of Technology, 2-12-1 Ookayama, Meguro-ku, Tokyo 152-8550, Japan.

- (1) (a) Feher, G.; Allen, J. P.; Okamura, M. Y.; Rees, D. C. *Nature* **1989**, *339*, 111–116. (b) Dieneshofer, J.; Michel, H. *Angew. Chem., Int. Ed.* **1989**, *28*, 829–847. (c) McDermott, G.; Prince, S. M.; Freer, A. A.; Hawthornthwaite-Lawless, A. M.; Papiz, M. Z.; Cogdell, R. J.; Isaacs, N. W. *Nature* **1995**, *374*, 517–521. (d) Stubbe, J.; Nocera, D. G.; Yee, C. S.; Chang, M. C. Y. *Chem. Rev.* **2003**, *103*, 2167–2202.
- (2) (a) Wasielewski, M. R. *Chem. Rev.* **1992**, *92*, 435–461. (b) Ward, M. D. *Chem. Soc. Rev.* **1997**, *26*, 365–375. (c) Tanaka, M.; Ohkubo, K.; Gros, C. P.; Guillard, R.; Fukuzumi, S. *J. Am. Chem. Soc.* **2006**, *128*, 14625–14633. (d) Fukuzumi, S.; Kojima, T. *J. Mater. Chem.* **2008**, *18*, 1427–1439.
- (3) Yoshizawa, M.; Miyagi, S.; Kawano, M.; Ishiguro, K.; Fujita, M. *J. Am. Chem. Soc.* **2004**, *126*, 9172–9173.

- (4) (a) Yoshizawa, M.; Fujita, M. *Pure Appl. Chem.* **2005**, *77*, 1107–1112. (b) Yoshizawa, M.; Tamura, M.; Fujita, M. *Science* **2006**, *312*, 251–254. (c) Furusawa, T.; Kawano, M.; Fujita, M. *Angew. Chem., Int. Ed.* **2007**, *46*, 5717–5719. (d) Nishioka, Y.; Yamaguchi, T.; Yoshizawa, M.; Fujita, M. *J. Am. Chem. Soc.* **2007**, *129*, 7000–7001. (e) Yamaguchi, T.; Fujita, M. *Angew. Chem., Int. Ed.* **2008**, *47*, 2067–2069.

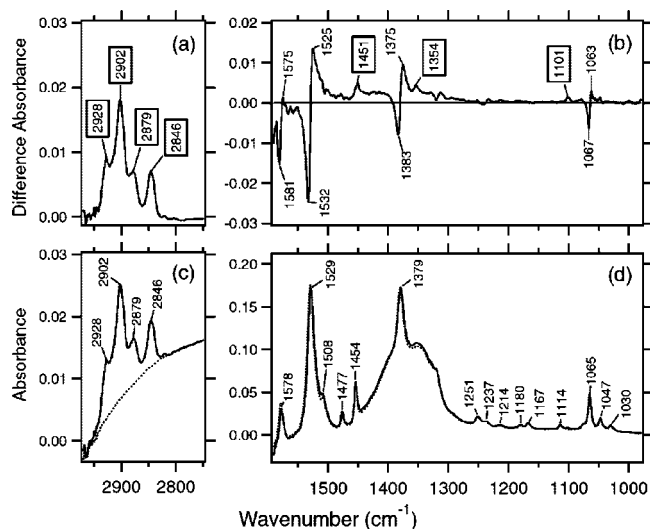


Figure 2. Difference IR spectra of Pd cage **1a** and complex **1a**⊃(**2**)₄ highlighting (a) the C–H region and (b) the fingerprint region. Overlay of the IR absorption spectra of **1a** (dotted lines) and **1a**⊃(**2**)₄ (solid lines) highlighting (c) the C–H region and (d) the fingerprint region. All of the spectra have been corrected for water absorption. The boxed tags indicate bands corresponding to the guest adamantane vibrations.

oxidized products, 1-adamantyl hydroperoxide and 1-adamantanol. The total yield of photoproducts per cage was ~24%, indicating that only one of the four guest adamantanes was oxidized. The proposed mechanism was based on several experimental results: (1) Under aerobic conditions, photolysis of **1**⊃(**2**)₄ in solution or the solid state produced an unusual blue color that immediately disappeared upon exposure to air or O₂. (2) The empty host and free guest are photochemically inert. (3) Changing the metal (from Pd²⁺ to Pt²⁺), counterions (from NO₃[−] to PF₆[−]), or solvent (from H₂O to CH₃CN) had no significant impact, but replacing the triazine core with benzene suppressed the photoreactivity. (4) During photolysis, a broad EPR signal from the blue solution was observed at *g* = 2.002. Finally, (5) experiments involving ¹⁸O labeling of O₂ or H₂O resulted in ¹⁸O incorporation into the oxidized products. These results indicated that photoreaction of **1**⊃(**2**)₄ is a cooperative reaction between the host and the guest and that the adamantyl radical is generated by a PET process. Therefore, the following sequence was proposed: (i) photoexcitation of a triazine chromophore increases its oxidative capability; (ii) electron transfer from the proximal adamantane to the triazine ligand, generating the adamantyl radical cation and the radical anion of **1**; and (iii) immediate trapping of the former by O₂ or H₂O to generate the oxidized products. In the oxidative photoreaction, cage **1** plays the role of sensitizer. Specifically, we deduced that the triazine group acts as the electron acceptor for PET.

Results and Discussion

Evidence of Host–Guest Interactions in the Infrared Spectra. An aqueous solution (3.4 mM) of **1a** and clathrate complex **1a**⊃(**2**)₄ was measured by FTIR spectroscopy, and strong host–guest interactions are evident (Figure 2). The boxed tags in the difference spectra indicate the new vibrational bands arising from the four adamantane guests, which are not present in the spectra of the empty Pd cage **1a** (the dotted lines in Figure 2c,d). The bands in the infrared region are attributable to the aromatic components of the Pd cage, i.e., the four panel ligands [2,4,6-tri(4-pyridyl)-1,3,5-triazine] and six Pd caps [2,2'-bipy-

ridine (bipy)]. The difference spectrum reveals the changes in the cage vibrational bands at 1529, 1379, and 1065 cm^{−1} and clearly indicates strong host–guest interactions. These bands are assigned to the panel ligand, as described later. Further support for the strong host–guest interactions is found in the X-ray crystal structure of **1a**⊃(**2**)₄. The four adamantane molecules are tightly packed inside the host cavity and separated from the triazine panel core by only 2.6 Å. The strong host–guest interactions present in the solution IR and solid X-ray data indicate that the host and guest are ideally situated to interact in the photoexcited state as well.

Vibrational Fingerprints for PET. A clear structural change in cage **1a** was observed by in situ IR spectroscopy when the 3.4 mM aqueous solution of clathrate complex **1a**⊃(**2**)₄ was UV-irradiated ($\lambda > 300$ nm) for 18 min. The difference IR spectra before and after UV irradiation feature three dominant negative peaks between 1050 and 1600 cm^{−1} (Figure 3). On the basis of density functional theory (DFT) vibrational analysis of the analogous cage **1b** (Figure 3a,c),⁵ the prominent negative peak at 1529 cm^{−1} is assigned to the C=N stretching vibration in the triazine ring ($\nu_{\text{calcd}} = 1528$ cm^{−1}). The negative peaks at 1379 and 1065 cm^{−1} are assigned to bending vibrations in the pyridine and triazine rings ($\nu_{\text{calcd}} = 1369$ cm^{−1}) and C–H bending vibrations in the pyridine rings ($\nu_{\text{calcd}} = 1067$ cm^{−1}), respectively. Thus, the spectroscopic changes can be attributed to structural changes solely in the triazine panel core.

The time-dependent difference IR spectrum confirmed that only one of the four adamantanes encapsulated in cage **1a** reacts. The absorption intensities of the vibrational bands at 1529, 1379, and 1065 cm^{−1} (assigned to the triazine panel) are each reduced by ~25% (Figure 4). Since there are four triazine panels, the loss of ~25% of the intensity implies that only one panel is affected by irradiation and PET. The formation of a single radical anion located on a single triazine panel is further supported by the fact that the total yield of oxidized adamantane (1-adamantyl hydroperoxide and 1-adamantanol) was 24% (or 96% assuming that only one guest is oxidized per cage).

The difference IR spectra show several relatively small positive bands (Figure 3). The panel molecule originally has *D*_{3h} symmetry, and according to DFT calculations [B3LYP/6-31G(d, p)++], the symmetry changes to *C*_{2v} upon radical anion formation because of the shortening of one of the single bonds connecting the triazine to a pyridine ring. The symmetry change permits the appearance of new, previously infrared-inactive modes of the panel molecule. Thus, the spectra of the radical anion should be different, and we ascribe the small positive bands to differences between the neutral and radical anion **1a** cages.

The C–H stretching vibrations of the adamantane guests are also affected by UV irradiation. In particular, the intensities of the bands at 2902, 2877, and 2843 cm^{−1} are significantly reduced by up to 60–70% (Figure 3b). However, only one adamantane molecule is actually oxidized upon UV irradiation of **1a**⊃(**2**)₄.³ The perturbation of the other three guest molecules is presumably due to symmetry breaking and rearrangement following the oxidation. The rearrangement and the loss of symmetry result in dramatic decreases in the intensities of the C–H stretching vibrations and/or upshifts in their frequencies. One is tentatively

(5) For the DFT calculations, analogue **1b** having ethylenediamine (en) instead of bipy as in **1a** was used as a model. Cage **1b** shows photoreactivity similar to that of **1a** as well as similar cage vibrational modes.

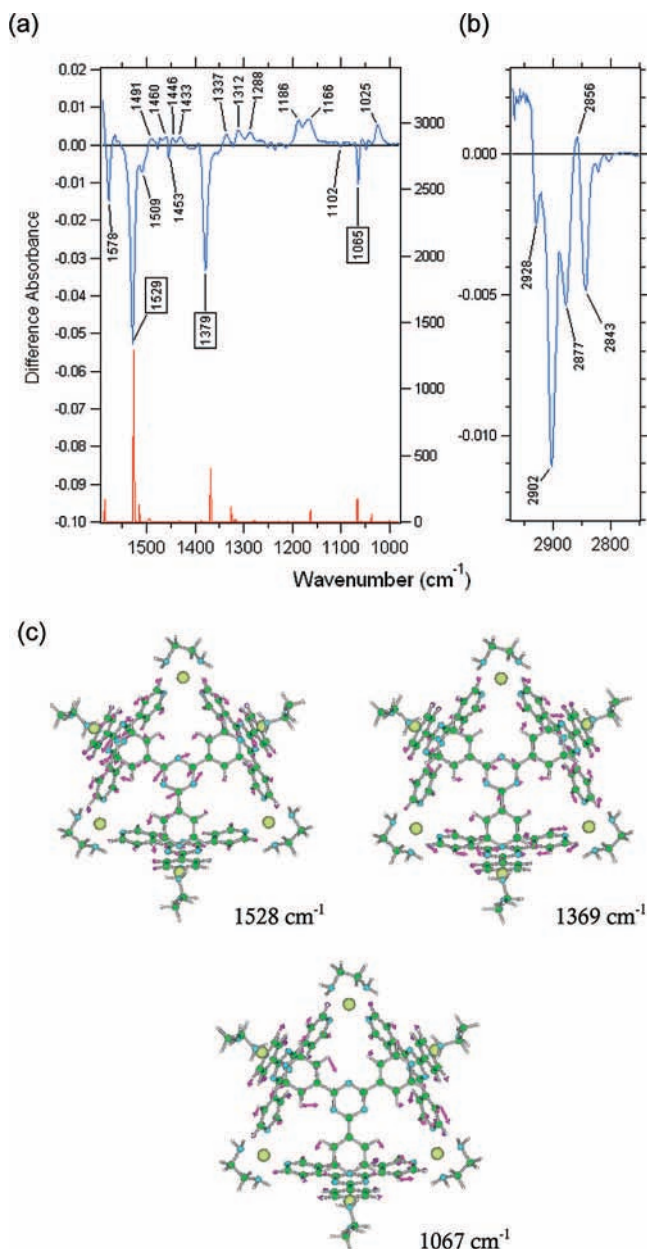


Figure 3. Difference IR spectra (before and after UV irradiation) of the aqueous solution of $1\mathbf{a}\supset(2)_4$ showing (a) the C–N vibrational region and (b) the C–H vibrational region. The calculated (DFT B3LYP/lanl2dz/6-31G) vibrational spectrum of cage $1\mathbf{b}$ is shown as red bars in (a) (scale factor = 0.985). (c) Calculated vibrational modes of $1\mathbf{b}$ at 1528, 1369, and 1067 cm^{-1} . Arrows indicate the directions and amplitudes of the vibrational motions of individual atoms.

assigned to the positive band at 2856 cm^{-1} , and the others are expected to fall outside the observation window.

Potential-Controlled UV–Vis Spectral Changes of a Self-Assembled Cage. Upon irradiation, the colorless solution of $1\mathbf{a}\supset(2)_4$ turned blue ($\lambda_{\text{max}} = 613 \text{ nm}$), indicating the generation of radical species (Figure 5). From the reduction in the triazine-panel vibrational intensities ($\sim 25\%$), we suggest that only one among four panels is structurally altered upon irradiation and participates in the PET upon irradiation of $1\mathbf{a}\supset(2)_4$. The electrochemical behavior of the clathrate complex also showed the reduction of only one ligand panel of the cage.

Pd cage $1\mathbf{a}$ proved to be unstable below -800 mV , showing irreversible redox waves. The Pt analogue $1\mathbf{c}$ showed similar

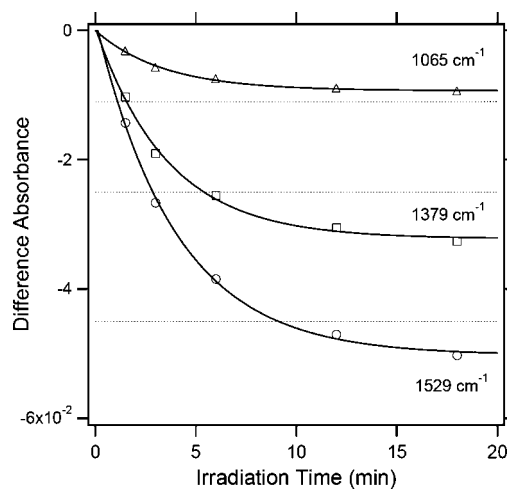


Figure 4. Reduction of absorbance intensity over time for the IR vibrational bands at (○) 1529, (□) 1379, and (△) 1065 cm^{-1} upon UV irradiation. The plots were obtained from spectra recorded at 1.5, 3, 6, 12, and 18 min. Each horizontal dotted line represents a quarter of the absorbance intensity for the corresponding frequency before irradiation, as calculated from Figure 2.

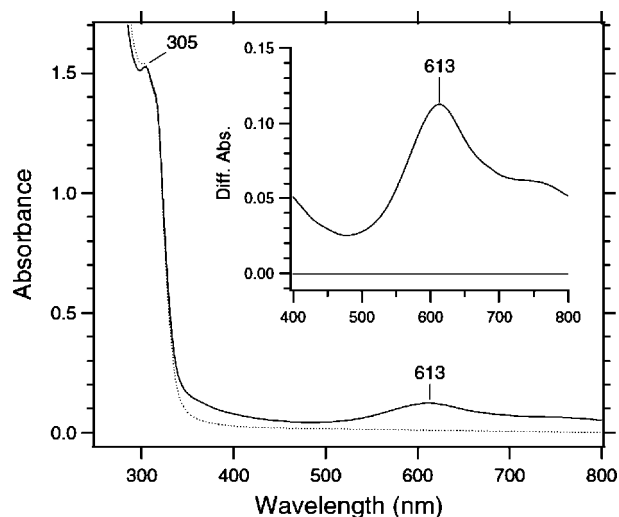


Figure 5. UV–vis absorption spectra of $1\mathbf{a}\supset(2)_4$ before and after UV irradiation. The spectra were measured before and after the FTIR experiments. The before-and-after difference spectrum is shown in the inset.

photochemistry and greater stability.³ The cyclic voltammogram of $1\mathbf{c}$ shows a reversible one-electron redox wave at -1017 mV ($E_{1/2}$ vs Ag/Ag^+ , $\text{Fc}^{0/+} = 108 \text{ mV}$) and pseudoreversible redox waves in the range from -1400 to -2000 mV corresponding to three electrons (Figure 6). The single-electron redox property of $1\mathbf{c}$ was confirmed by coulometry at -1300 mV . It is important to note that no simultaneous four-electron reduction, which would have been indicative of electronically independent ligand panels, was observed. The four panels are electronically coupled to each other through the Pt ion centers.⁶

The potential-controlled UV–vis–NIR spectra of $1\mathbf{c}$ show a broad band between 600 and 1200 nm (Figure 7), similar to the photoirradiated solution spectra of $1\mathbf{c}\supset(2)_4$.^{3,7} By analogy, the blue radical species observed in the photoirradiated solution of $1\mathbf{a}\supset(2)_4$ is also assigned as the single-electron-reduced form of cage 1 .

(6) (a) Ruben, M.; Breuning, E.; Gisselbrecht, P.; Lehn, J. M. *Angew. Chem., Int. Ed.* **2000**, *39*, 4139–4142. (b) Ruben, M.; Lehn, J. M.; Muller, P. *Chem. Soc. Rev.* **2006**, *35*, 1056–1067.

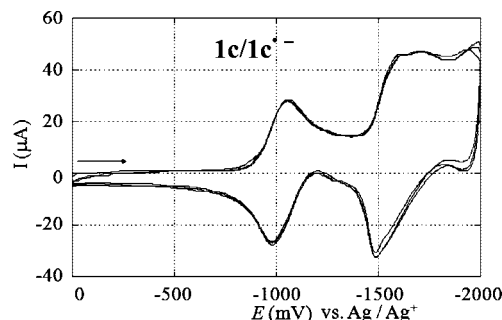


Figure 6. Cyclic voltammogram of the Pt analogue **1c** in CH_3CN (0.5 mM). The half-wave potential of the first redox wave was $E_{1/2} = -1017$ mV. Conditions: electrolyte, 50 mM $\text{TBA}^+\text{PF}_6^-$; Ar bubbling for 15 min; sweep rate, 100 mV/s.

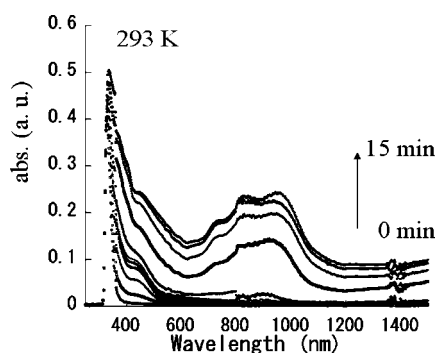


Figure 7. UV–vis–NIR spectra during bulk electrolysis of 0.25 mM $\{[(\text{en})\text{Pt}]_6(\text{TPT})_4\}(\text{PF}_6)_{12}$ in CH_3CN at -1300 mV vs Ag/Ag^+ for 15 min under an Ar atmosphere. Electrolyte: 50 mM $\text{TBA}^+\text{PF}_6^-$.

Theoretical Support for an Electron-Acceptor Triazine. The single-electron-accepting character of **1a** is supported by DFT calculations. The HOMO to HOMO–5 and the nearly degenerate LUMO to LUMO+7 are mainly dominated by the Pd d_{z^2} orbitals and the π^* orbitals of the triazine panels, respectively. The energy diagram suggests that upon one-electron reduction of **1a**, an electron is placed in the π^* orbital of a triazine panel (Figure 8). The first eight unoccupied molecular orbitals (MOs) are degenerate (within 0.03 eV), and once an electron is placed in the LUMO, the energy levels of the remaining unoccupied MOs should increase considerably, causing the energy cost to accommodate a second electron in the LUMO+1 to be much greater. Although there is no direct π conjugation between the panels in cage **1a**, the initial single-electron redox wave at -1017 mV in the cyclic voltammogram indicates that there is electronic communication between the cage panels.

Conclusion

The PET process in the remarkable photooxidation of alkanes in the self-assembled cage **1** was examined through in situ IR and UV spectroscopy, electrochemistry, and theoretical calcula-

(7) UV irradiation of adamantane encapsulated within a Pd or Pt cage produced a blue solution. On exposure of the blue solution to air, the visible-region absorption bands disappeared simultaneously, which indicates that a reactive species was generated at room temperature. Although the potential-controlled UV–vis spectrum of the one-electron-reduced empty Pt cage contains very similar broad absorption bands from 700 to 1000 nm, no band appears at ~ 600 nm (Figure 7). Therefore, we presume that the 600 nm absorption band in Figure 5 is derived from a reactive intermediate produced by the redox reaction of the cage with adamantane or the effect of stabilization of the SOMO of the anion radical of the cage by interactions with an oxidized product of adamantane, such as 1-adamantanol or 1-adamantyl hydroperoxide.

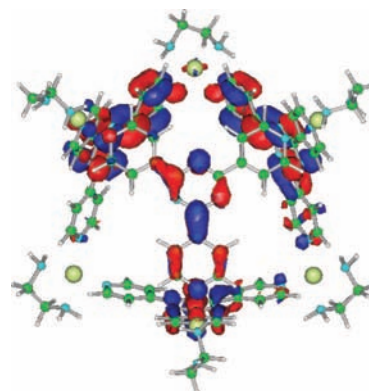


Figure 8. LUMO of the cation cage in **1b** calculated at the DFT B3LYP/lanl2dz/6-31G level of theory.

tions. The clathrate complex $\mathbf{1}\supset(\mathbf{2})_4$ is unique and particularly well-suited for guest-to-host PET. First, the triazine core of the panel ligands is very electron-poor because of the three coordinated pyridine moieties and thus is a good electron acceptor. Second, the four guest molecules are tightly bound and packed within the cage cavity. As a result of this cage effect, the adamantane molecules are held in very close proximity to the triazine panels, facilitating the unusual PET. In view of the electronic nature of cage **1**, it is expected that exploiting the cage effect will enable the development of new and potentially useful reactions via PET in the cavity of **1**.

Experimental Section

Materials. Solvents and reagents were purchased from TCI, WAKO Pure Chemical Industries, and Aldrich Chemical and used without any further purification. The preparation of **1a**, **1b**, and **1c** is described in previous reports.⁸

FT-IR Spectroscopy. Samples (100 μL) of 3.4 mM solutions of **1a** and $\mathbf{1a}\supset(\mathbf{2})_4$ were bubbled with nitrogen gas for 10 min, after which an 8 μL aliquot of each sample was sealed by two BaF_2 windows ($\phi = 18$ mm) with a Teflon spacer (50 μm thickness). Each sample was placed in a holder that was mounted in a cryostat (Optistat DN, Oxford Instruments) placed in an FT-IR spectrometer (FTS-7000, DIGILAB). The ambient air in the spectrometer and the sample chamber was replaced with N_2 and He gas, respectively. The temperature of the sample holder was kept at 277 K. Each spectrum was measured with 2 cm^{-1} resolution and constructed from 256 interferograms. To extract the absorption spectra of **1a** and $\mathbf{1a}\supset(\mathbf{2})_4$, the reference spectrum of water was collected just before the measurement of the sample solution. In the light-induced difference IR spectroscopic measurements, a xenon lamp with an optical filter (>300 nm) (MAX-301, Asahi Spectra Co., Ltd., Japan) was used as the light source for illumination. The difference spectrum was obtained by subtraction of spectra taken before and after the illumination. Three spectra obtained in this way were averaged to give the UV-light induced difference spectrum.

ATR–FTIR Spectroscopy. Aqueous solutions of cage **1a**, (bipy) $\text{Pd}(\text{NO}_3)_2$, and TPT dissolved in hexane were dried on a diamond internal reflection element (nine-bounce type) of an ATR accessory (DurasamplIR II, Smiths Detection), which was placed in an FT-IR spectrometer (FTS-6000, Bio-Rad). Each spectrum was measured at room temperature and constructed from 128 interferograms with 2 cm^{-1} resolution.

UV–Vis Spectroscopy. The UV–vis absorption spectra were measured using a UV–vis spectrometer (V-550DS, JASCO)

(8) (a) Yoshizawa, M.; Kusukawa, T.; Fujita, M.; Yamaguchi, K. *J. Am. Chem. Soc.* **2000**, *122*, 6311–6312. (b) Kusukawa, T.; Fujita, M. *J. Am. Chem. Soc.* **2002**, *124*, 13576–13582.

equipped with the same cryostat as used in the FT-IR spectrometer, enabling the use of the same sample holder. Therefore, the absorption spectrum of **1a**(**2**)₄ was measured before and after the FT-IR experiment without detaching the sample window.

Potential-Controlled UV–Vis Spectroscopy of {[*(en)*Pt]₆(TPT)₄}(PF₆)₁₂. UV–vis spectra were recorded on SHIMADZU UV-3150 using a cell with 1 mm width in H₂O with 1 cm length. The electrochemical experiments were performed with a BAS100B/W electrochemical analyzer (Bioanalytical Systems). A glassy carbon working electrode (7 mm²), a Pt counter electrode, and a Ag⁺/AgCl reference electrode were utilized in a single-component cell. The working electrode was polished with 0.05 μm alumina on a felt surface and rinsed with water prior to every measurement. All

of the samples for cyclic voltammetry were bubbled with Ar gas for 15 min to exclude oxygen before the measurements.

Acknowledgment. This research was partially supported by the Ministry of Education, Culture, Sports, Science and Technology of Japan (20050013 to Y.F.).

Supporting Information Available: ATR–FTIR spectra and results of electrochemical experiments and theoretical calculations. This material is available free of charge via the Internet at <http://pubs.acs.org>.

JA8089075